Chemometrics and elemental mapping by portable LIBS to identify the impact of volcanogenic and non-volcanogenic degradation sources on the mural paintings of Pompeii

Silvia Pérez-Diez,[a,*] Luis Javier Fernández-Menéndez,[b] Marco Veneranda,[a,c] Héctor

Morillas,[a,d] Nagore Prieto-Taboada,[a,e] Silvia Fdez-Ortiz de Vallejuelo,[a] Nerea Bordel,[b]

Alberta Martellone,[f] Bruno De Nigris,[f] Massimo Osanna,[g] Juan Manuel Madariaga,[a,h] and

Maite Maguregui[i,*]

[a]Department of Analytical Chemistry, Faculty of Science and Technology, University of the Basque Country

UPV/EHU, Bilbao, Spain

[b]Department of Physics, Faculty of Sciences, University of Oviedo, Oviedo, Spain

[c] Department of Condensed Matter Physics, Crystallography and Mineralogy, University of Valladolid,

Valladolid, Spain

[d]Department of Didactic of Mathematics and Experimental Sciences, Faculty of Education and Sport,

University of the Basque Country UPV/EHU, Vitoria-Gasteiz, Spain

[e]Department of Applied Chemistry, Faculty of Chemistry, University of the Basque Country UPV/EHU, Donostia,

Spain.

[f]Applied Research Laboratory of Archaeological Park of Pompeii, via Plinio 4, Pompeii, Italy

[g]General Director of Archaeological Park of Pompeii, via Plinio 4, Pompeii, Italy

[h]UNESCO Chair of Cultural Landscapes and Heritage, University of the Basque Country UPV/EHU, Vitoria-Gasteiz,

Spain

[i]Department of Analytical Chemistry, Faculty of Pharmacy, University of the Basque Country UPV/EHU,

Vitoria-Gasteiz, Spain

*Corresponding authors: silvia.perezd@ehu.eus, maite.maguregui@ehu.eus

Supplementary Material

Supplementary Figures

Fig. S1 to Fig. S19

Supplementary Tables

Tables S1 to S8

2. EXPERIMENTAL SECTION

2.1. Mural paintings and samples under study

Table S1. Points and samples analyzed at the House of Ariadne (ARI) by LIBS, HH-EDXRF and Raman.

	LIBS	HH-EDXRF	Walls analyzed by Raman spectroscopy	Samples
Basement	ARI_B:1-36	ARI_B:1-36	Published in a previous work [1]	M0 (corresponding to ARI_B-36) M1 (corresponding to ARI_B-9) M2 (corresponding to ARI_B-25) M3 (corresponding to ARI_B-8)
Room 17	ARI_17:1-17	ARI_17:1-17	Lower southern wall: ARI_17	No samples
	ARI_17B:1-9	ARI_17B:1-9	Upper west wall: ARI_17B	

Table S2. Points analyzed at the House of the Golden Cupids (GC) by LIBS, HH-EDXRF and Raman.

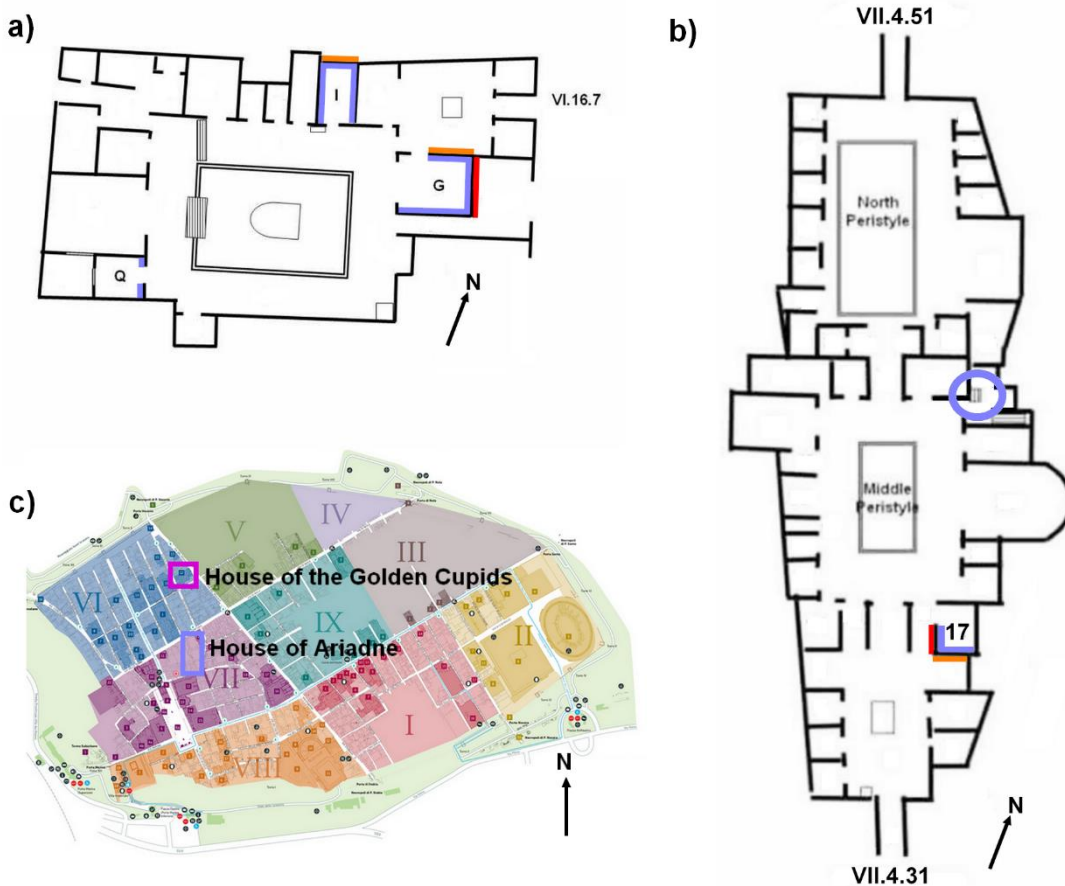|	LIBS	XRF	Walls analyzed by Raman spectroscopy
Room G	GC_G:1-103	GC_G:1-51, 91-103 (central panel, eastern wall)	Northern (corresponding to GC_G:61-69), eastern (corresponding to GC_G:1-51, 91-103) and southern wall (corresponding to GC_G:70-90)
Room I	GC_I:1-49	-	Western (corresponding to GC_I:39-42), northern (corresponding to GC_I:26-38) and eastern wall (corresponding to GC_I:1-25)
Room Q	GC_Q:37-48	GC_Q:37-48	East wall (corresponding to GC_Q:37-48)

Fig. S1. A) Plan of the House of the Golden Cupids (Regio VI, 16, 7), extracted from Pompeii in Pictures [2]. Walls marked in blue were analyzed for this study, all corresponding to roof-protected rooms. Walls marked in orange and red have their rear exposed to environmental impact: orange corresponds to improbable direct rainfall and red corresponds to rainfall risk in case of south-southwest wind. B) Plan of the House of Ariadne (Regio VII, 4, 31/51), extracted from Pompeii in Pictures [2]. Walls marked in blue were analyzed for this study, corresponding to a roof-protected room. Blue circle marks the stairs that lead to the underground basement considered in this work. Walls marked in orange and red have their rear exposed to environmental impact: orange corresponds to improbable direct rainfall and red corresponds to rainfall risk in case of north-northeast wind. C) Map of the Archaeological Park of Pompeii, extracted from Pompeii Sites [3], showing the location of the House of the Golden Cupids and the House of Ariadne.

Fig. S2. Sampling locations at the basement of the House of Ariadne.

Fig. S3. Points (ARI_B:1-36) of the basement of the House of Ariadne analyzed by LIBS and HH-EDXRF.
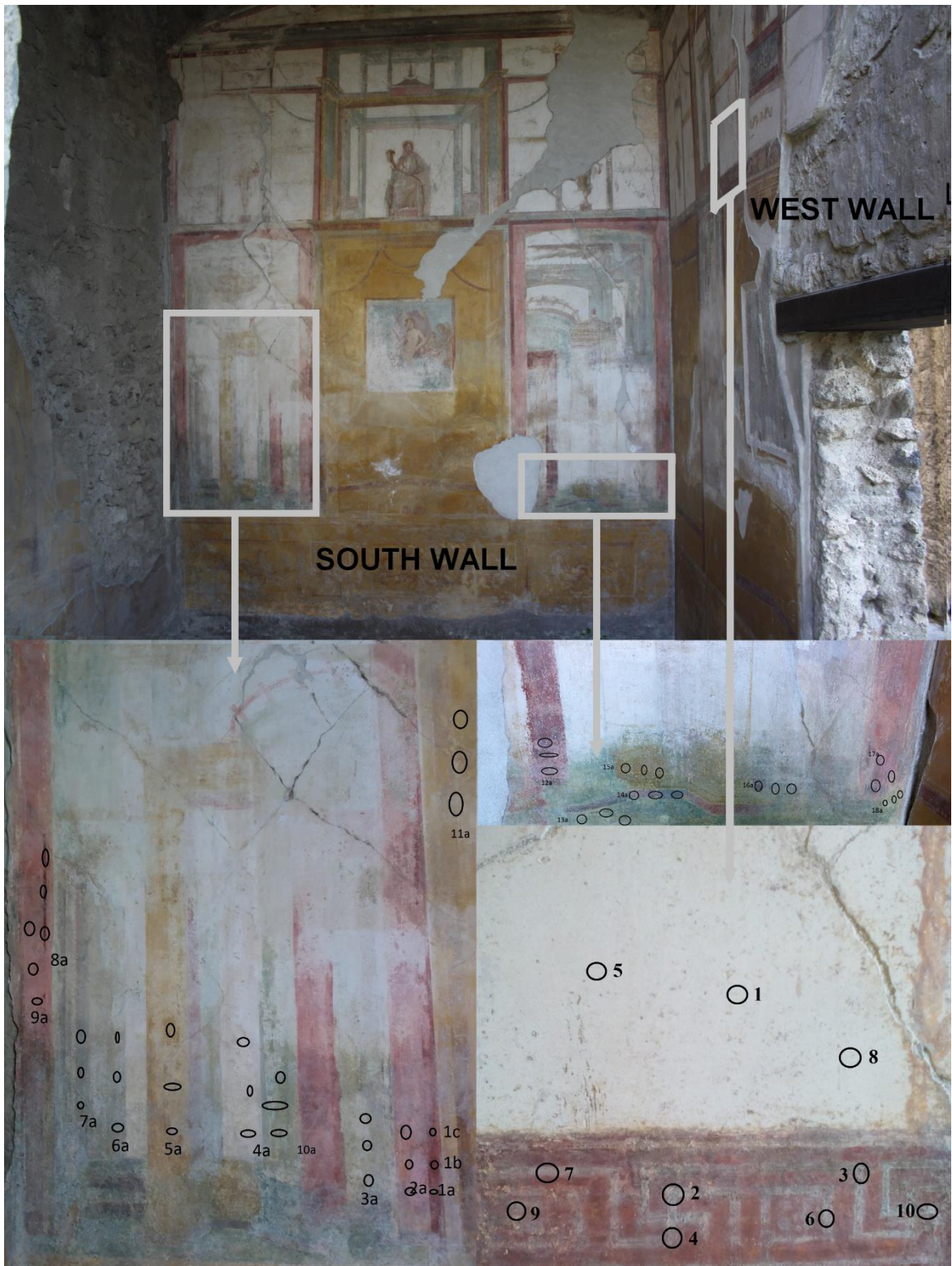
Fig. S4. Points of the lower southern wall (ARI_17:1-11; ARI_17:12-17) and the upper west wall (ARI_17B:1-9) of Room 17 of the House of Ariadne analyzed by LIBS, HH-EDXRF and Raman.

Fig. S5. Northern, eastern and southern wall of Room G of the House of the Golden Cupids. The marked areas on each wall correspond to the analyzed areas detailed on Fig. S6 to S8. A further area of the southern wall, out of view, was also analyzed (Fig. S8B).

Fig. S6. Points (GC_G:61-69) of the northern wall of Room G of the House of the Golden Cupids analyzed by LIBS and Raman.

Fig. S7. Points (central panel: GC_G:1-51, 91-103) of the eastern wall of Room G of the House of the Golden Cupids analyzed by LIBS, HH-EDXRF and Raman.

Fig. S8. A) Points GC_G:82-90 of the *predella* of the southern wall of Room G of the House of the Golden Cupids analyzed by LIBS and Raman. B) Points GC_G:70-81 of the southern wall of Room G of the House of the Golden Cupids analyzed by LIBS and Raman. This area is not highlighted in

Fig. S5, since its location goes beyond the right part of the panoramic image.

Fig. S9. Points of the western (GC_I:39-42), northern (GC_I:26-38) and eastern wall (GC_I:1-25) of Room I of the House of the Golden Cupids analyzed by LIBS and Raman.

2.2. Instrumentation

The XMET5100 (Oxford Instruments, UK) HH-EDXRF instrument used in this work is equipped with a Rh X-Ray tube working at a maximum voltage of 45 kV. The size of the emitted X-Ray beam is 9 mm. The analyzer includes a silicon drift detector (SDD) of high resolution that is able to provide an energy resolution of 150 eV (FWHM of the Mn K_α line). Besides, the analyzer contains a PDA to control the spectrometer and save the spectral and quantitative information. To improve the limit of detection (LOD), the spectra were acquired during 100 s (real time) and the voltage and current of the X-Ray tube was set at 45 kV and 15 µA respectively. In order to improve the detection of Cl, lower voltage (13 kV) and higher current (45 µA) was also used.

For the in situ Raman analysis, a portable innoRam™ Raman spectrometer (B&WTEK$_{INC.}$, Newark, USA) provided with a CleanLaze® technology 785 nm excitation laser (<300 mW laser output power) was used. The instrument implements a controller of the laser power (a scale from 0 to 100% of the total power of the laser). It also includes a two dimensional charge coupled device (CCD) to detect the dispersed Raman signal, which is Thermoelectric Cooled (TC) to −20 °C to maximize the dynamic range by reducing dark current. A back-thinned CCD is used to obtain 90% quantum efficiency via collection of incoming photons at wavelengths that would not pass through a front illuminated CCD. A spectral resolution of 4.0 cm^{-1} (measured at 912 nm) can be achieved with a double pass transmission optic. The spectra were acquired between 65 and 3000 cm^{-1}. The spectral acquisition and data treatment was performed using the BWSpec™ v.4.0215 (B&WTEKINC., Newark, USA) and OMNIC 7.2 (Thermo, Massachusetts, USA) software.

SEM-EDS analyses were performed using a X-Max energy dispersive X-ray spectrometer (Oxford Instruments, Abingdon, Oxfordshire, U.K.) coupled to an EVO40 scanning electron microscope (Carl Zeiss NTS GmbH, Germany). The elemental analysis was carried out using a 8.5-mm working distance, a 35° takeoff angle, and an acceleration voltage of 30 kV. An integration time of 50 s was employed to improve the signal-to-noise ratio of EDS spectra. The spectral data treatment was carried out using the INCA software (Oxford Instruments, Abingdon, Oxfordshire, U.K.), able to offer a semi-quantitative approach of the elements present in the sample under study.

The quantification of the ions present in rainwater and groundwater samples were conducted using a Dionex ICS 2500 ion chromatograph equipped with an ED50 conductivity detector and an AS 40 auto sampler. Ion quantification was carried out by means of external calibration curves, using 1000 mg·L^{-1} standard solutions (Fluka Sigma Aldrich) of the ions detected in the samples. The separation of anions was carried out using an IonPac AS23 (4 × 250 mm) column, an IonPac AG23 (4 × 50 mm) pre-column, 4.5 mM Na_2CO_3/0.8 mM $NaHCO_3$ mobile phase, 25 mA suppression current and 1 mL·min^{-1} flow. The separation of cations was carried out using an IonPac CS12A (4 × 250 mm) column and IonPac CG-12A (4 × 50 mm) precolumn from Vertex, 20 mM CH_4SO_3 mobile phase, 50 mA suppression current and and 1 mL·min^{-1} flow. Finally, data processing was performed using 6.60-SPIA CHROMALEON software (Dionex Corporation, USA).

A Modular OCT Scanhead Thorlabs OCTP Series was used to acquire images of a fresco painting mock-up and to measure the craters left by the LIBS measurements (5 and 30 laser pulses). The equipment is based on a swept source with a wavelength of ~1300 nm. The system provides a resolution in air of 12 μm axial and 25 μm transverse, giving a maximum penetration in air conditions of 3 and 10 mm width.

The PHREEQC software was employed to estimate the different salt crystallization mechanisms, including the crystallization pressure and the saturation indices. The calculations were based on the Wateq4f database. The thermodynamic modeling was executed on the concentrations values obtained via ion chromatography for the samples of rain- and groundwater, considered as multicomponent aqueous solutions with the following systems: Na^+– K^+–Ca^{2+}–Mg^{2+}–F^-–Cl^-–NO_3^-–SO_4^{2-}. The calculations were run both at 10 and 25 ºC and charge was balanced through alkalinity.

2.3. Materials

Biocalce® Pietra and Biocalce® Intonachino Fino were purchased from Kerakoll in order to prepare fresco mock-ups. Biocalce® Pietra was left to set as the *arriccio*, whereas Biocalce® Intonachino Fino was extended as the *intonaco* and painted with pigment dispersed in water. Two sets of laser pulses (5 and 30) were performed on the mock-up to replicate the experimental conditions on the mural paintings of the Archaeological Park of Pompeii and to evaluate the penetration depth.

3. RESULTS AND DISCUSSION

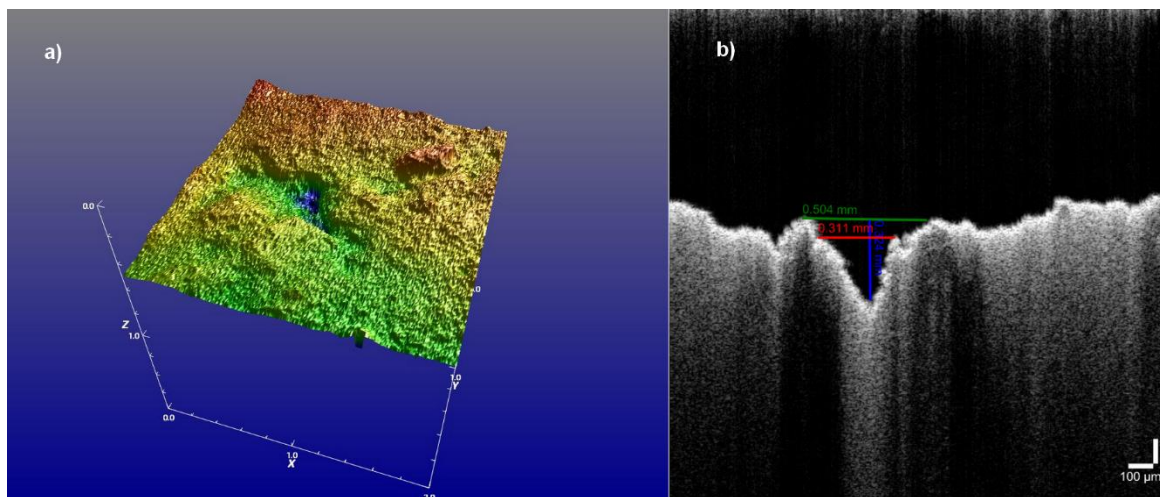## 3.1. Halogens and alkali metals detection by portable LIBS on Pompeian mural paintings

Fig. S10. A) 3D image of a 30 laser pulses crater on the surface of the fresco mock-up. B) OCT measurement of the crater dimensions.
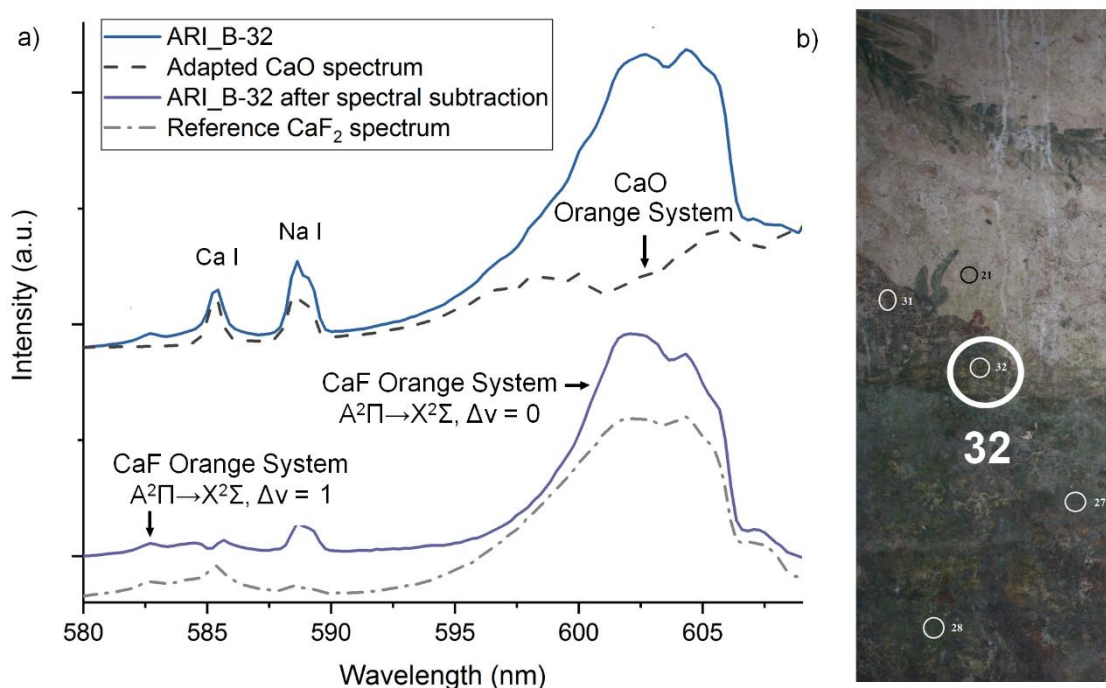
Fig. S11. A) LIBS spectrum of point 32 of the mural painting from the basement of the House of Ariadne (ARI_B-32), the adapted CaO spectrum and the result of the subtraction of the CaO spectrum to ARI_B-32, compared to a reference spectrum of a pressed pellet of pure CaF_2. The spectra show the atomic emission lines of Ca I (585.75 nm) and Na I (589.00 and 589.58 nm, unresolved). B) Location of the measured point in the mural painting.

Both the non-interfered signal at 583.00 nm and the series of signals around 600 nm of the CaF orange system are visible in Fig. S11. The weakness of the 583.00 nm signal implies that it can be absent in points with low concentration of F, in which the only observable system is the CaF emission around 600 nm after the CaO subtraction (see Fig. S12). Hence, the latter is preferred for integration after the CaO subtraction [4].
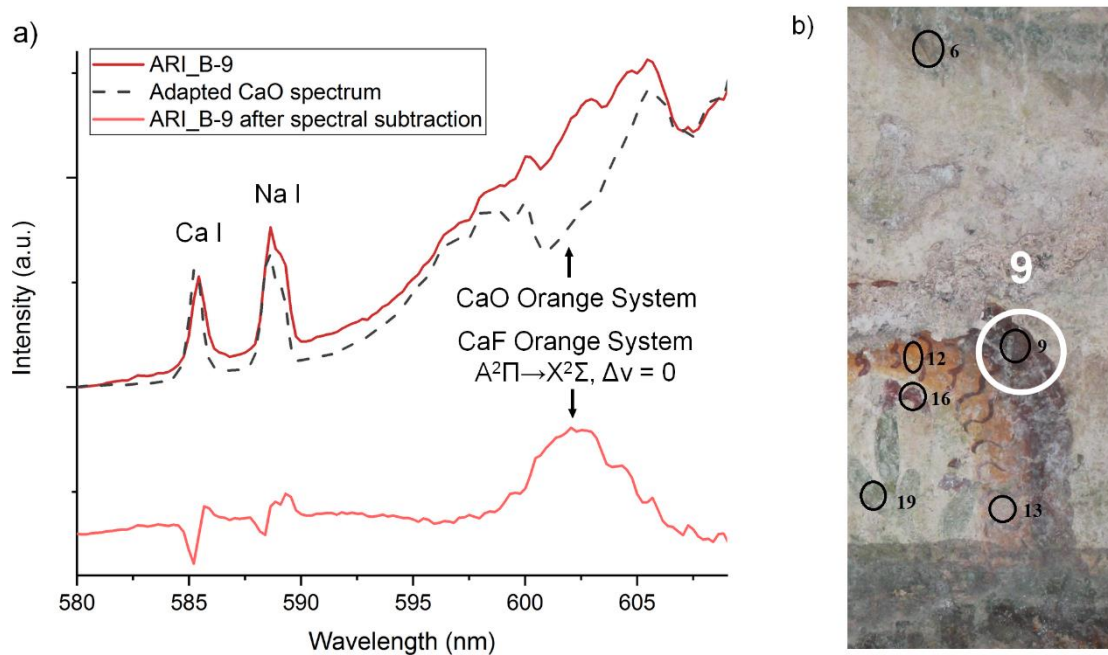
Fig. S12. A) LIBS spectrum of the point 9 of the mural painting from the basement of the House of Ariadne (ARI_B-9), the adapted CaO spectrum and the result of the subtraction of the CaO spectrum to ARI_B-9. The spectra show the atomic emission lines of Ca I (585.75 nm) and Na I (589.00 and 589.58 nm, unresolved). B) Location of the measured point in the mural painting.
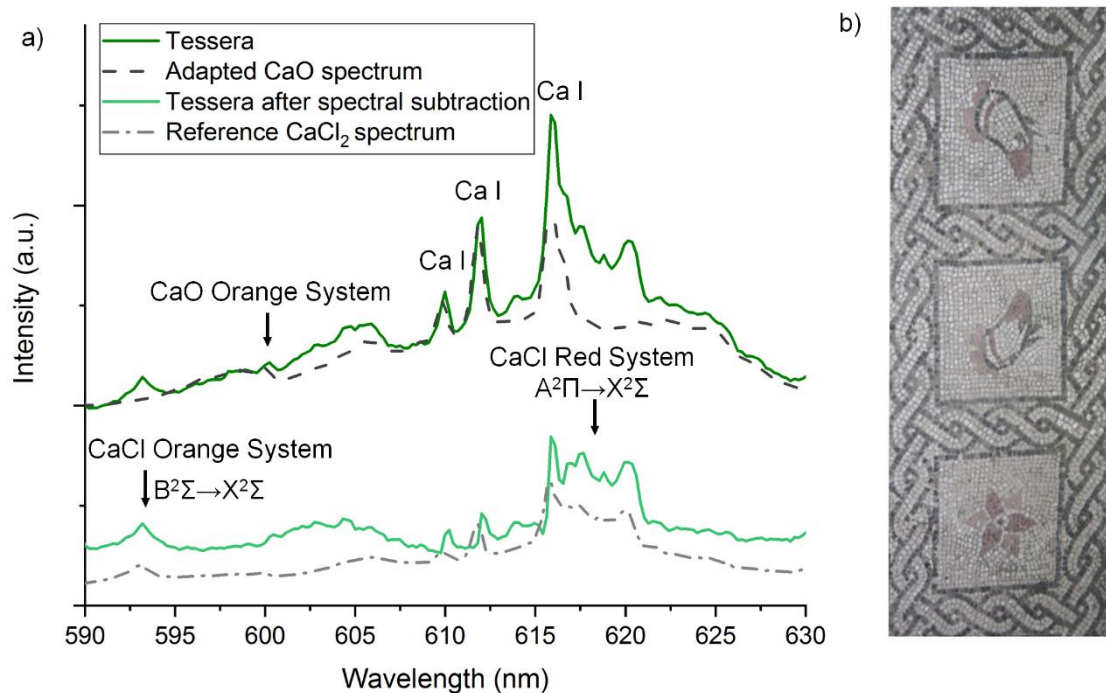
Fig. S13. A) LIBS spectrum of the CaCl orange and red systems acquired on one of the tesserae from the mosaic of the Room E of the House of Golden Cupids, the adapted CaO spectrum and the result of the subtraction of the CaO spectrum to the spectrum of the tessera, compared to a reference spectrum obtained on a pressed pellet of pure $CaCl_2$. The spectra show the atomic emission lines of Ca I (610.25, 612.21 and 616.21 nm). B) Tesserae of the mosaic of Room E (House of the Golden Cupids).

3.2. Halogens and alkali metals distribution on the mural paintings of the basement of the House of Ariadne
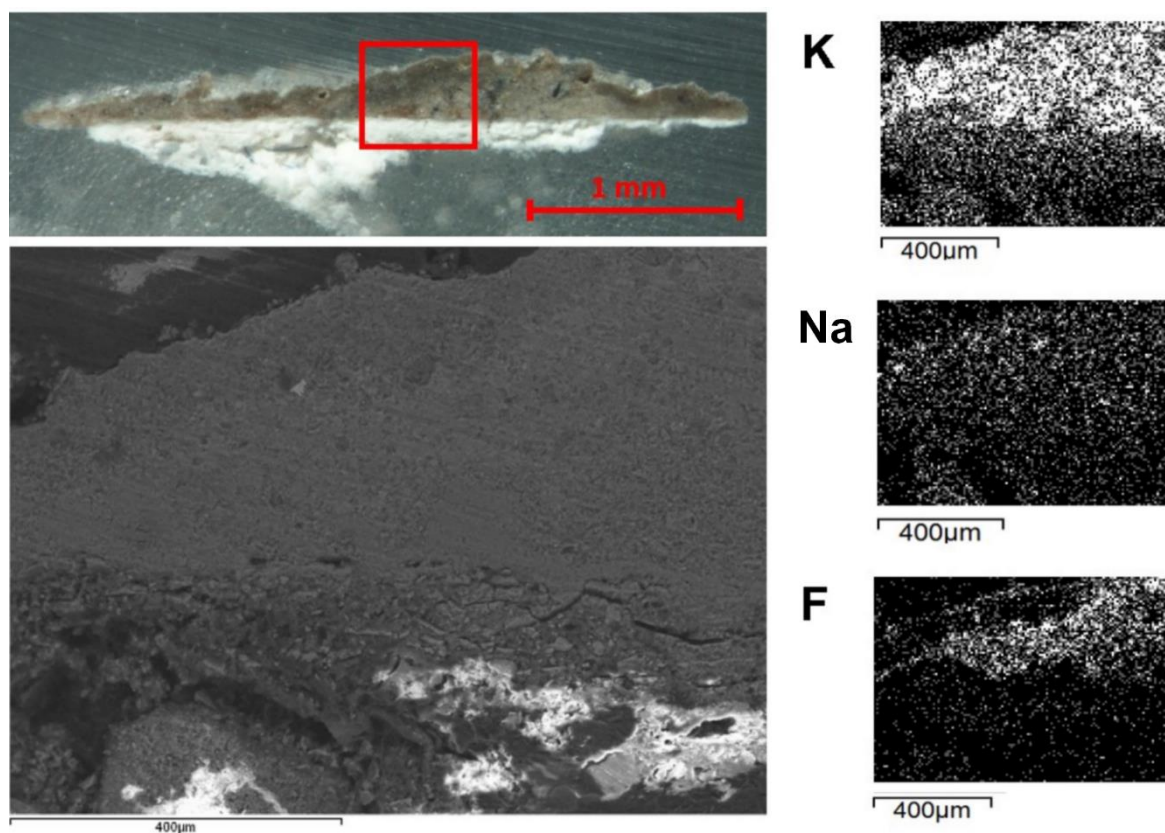

Fig. S14. SEM images of the M0 sample stratigraphy with the pyroclastic deposit marked with the red square and a zoom of this area, together with the elemental distribution maps of K, Na and F in this mapped area. The distribution map of Cl is not shown due to the contribution of the resin employed to embed the sample as cross section.

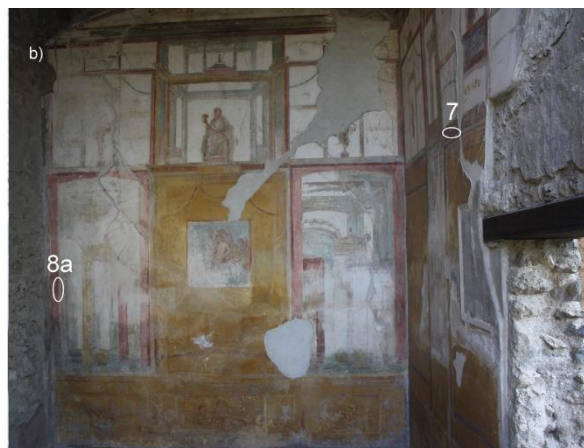## 3.3. Halogens and alkali metals distribution on the mural paintings of the House of the Golden Cupids
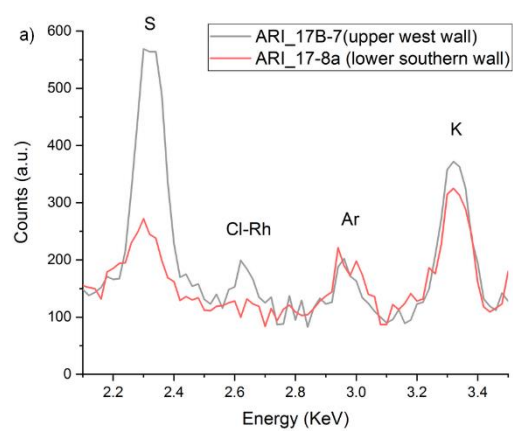

Fig. S15. A) HH-EDXRF spectra of two in situ analyzed points of Room 17 (*oecus*) of the House of Ariadne. The upper part of the west wall (ARI_17B-7) shows Cl, while the lower part of the southern wall lacks of this element (ARI_17-8a). B) Location of the analyzed points in the Room 17 of the House of Ariadne.

Fig. S16. Qualitative LIBS distribution image of Na of Room G of the House of the Golden Cupids. Vertical wide lines mark the separation of the north, eastern and south walls. A) North and eastern wall. B) Southern wall. Red areas correspond to the points with higher relative net intensities of Na, while green areas correspond to lower relative net intensities.
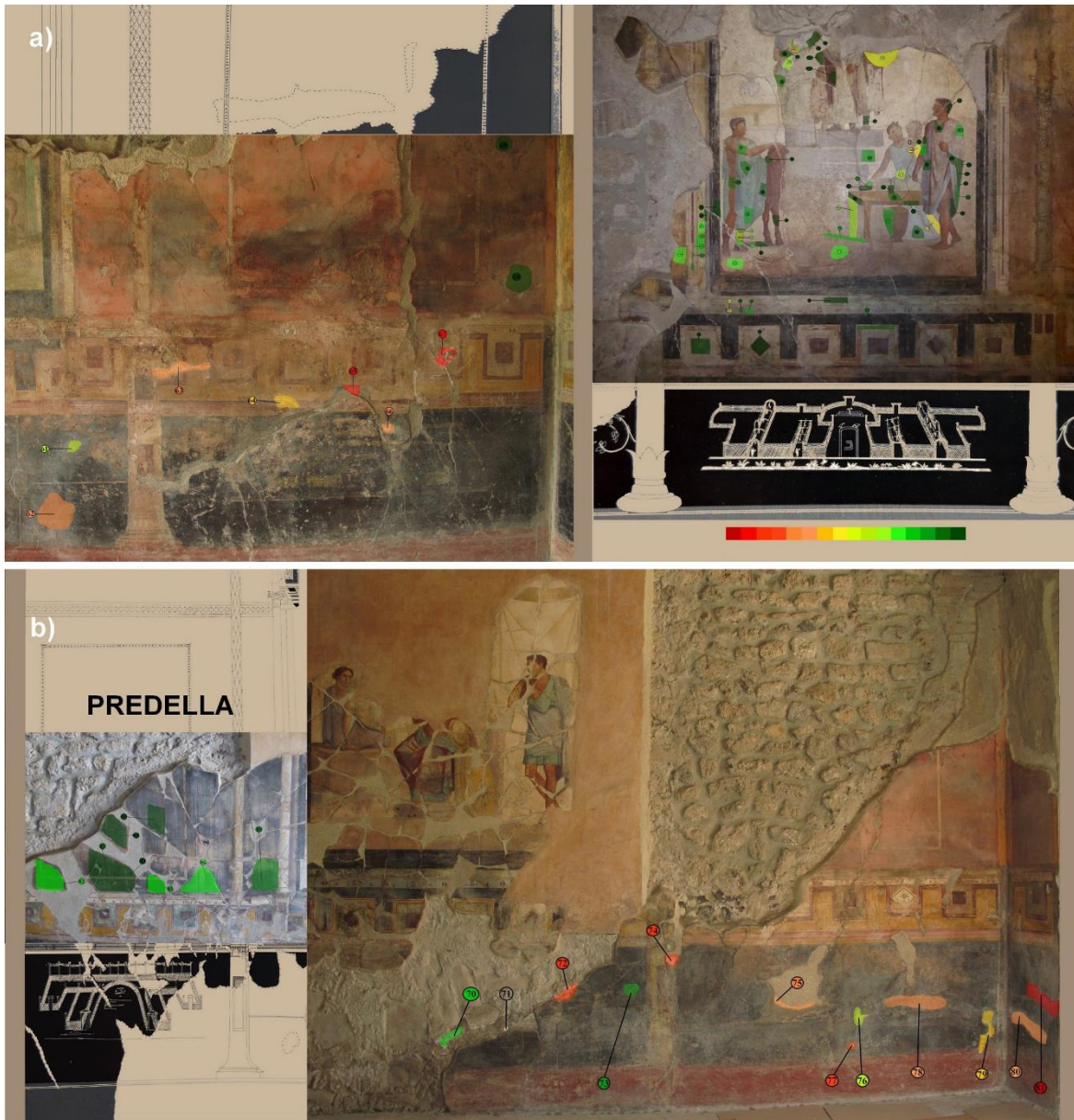
Fig. S17. Qualitative LIBS distribution image of K of Room G of the House of the Golden Cupids. Vertical wide lines mark the separation of the north, eastern and south walls. A) North and eastern wall. B) Southern wall. Red areas correspond to the points with higher relative net intensities of K, while green areas correspond to lower relative net intensities.
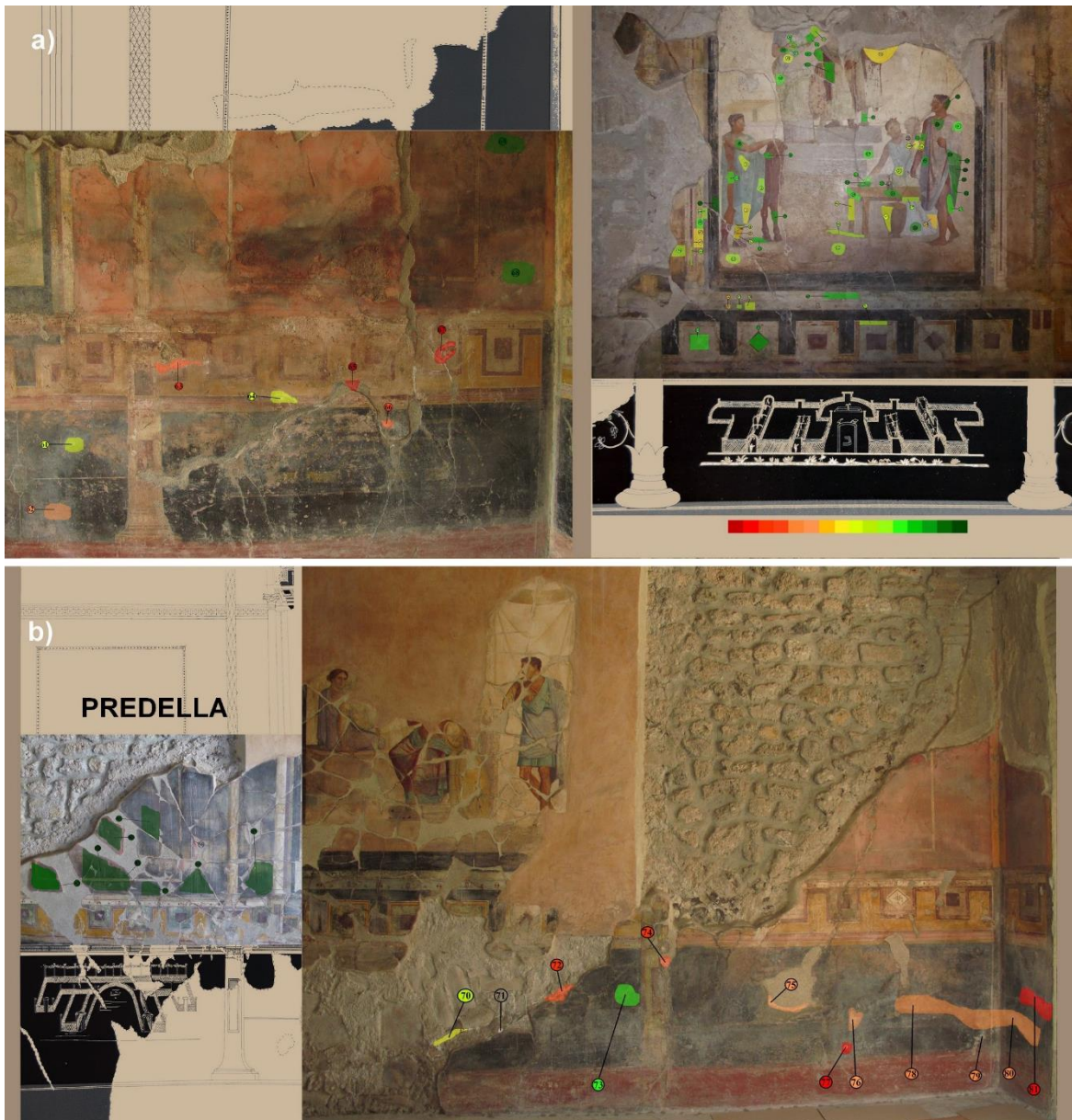
Table S3. Selection of the highest LIBS intensities of CaCl on Room G of the House of the Golden Cupids.

Points	Location	CaCl (a.u.)
GC_G-85	*Predella* (southern wall)	3193
GC_G-82	*Predella* (southern wall)	2184
GC_G-83	*Predella* (southern wall)	1915
GC_G-84	*Predella* (southern wall)	1755
GC_G-89	*Predella* (southern wall)	1597
GC_G-98	Central panel (eastern wall)	1500
GC_G-101	Central panel (eastern wall)	1271
GC_G-100	Central panel (eastern wall)	1268
GC_G-13	Central panel (eastern wall)	1128
GC_G-94	Central panel (eastern wall)	1123
GC_G-91	Central panel (eastern wall)	1097
GC_G-41	Central panel (eastern wall)	1027
GC_G-15	Central panel (eastern wall)	1000
GC_G-86	*Predella* (southern wall)	956
GC_G-32	Central panel (eastern wall)	895
GC_G-6	Central panel (eastern wall)	872
GC_G-5	Central panel (eastern wall)	818
GC_G-88	*Predella* (southern wall)	811
GC_G-87	*Predella* (southern wall)	798

Fig. S18. A) Points GC_Q:44-47, analyzed by LIBS, HH-EDXRF and Raman spectroscopy at the eastern wall of Room Q of the House of the Golden Cupids. B) and C) Details of efflorescence GC_Q-46.

Table S4. LIBS intensities of Na, K and CaF on the efflorescences of Room Q of the House of the Golden Cupids.

Points	Na I (a.u.)	K I (a.u.)	CaF (a.u.)
GC_Q-37	59214	47574	0
GC_Q-39	78705	387840	58468
GC_Q-39	47500	90932	0
GC_Q-40	37626	142898	0
GC_Q-41	70295	280545	22340
GC_Q-42	3308	9930	27538
GC_Q-43	6899	20221	97784
GC_Q-44	74381	178063	0
GC_Q-45	49889	68953	0
GC_Q-46	39515	215421	14049
GC_Q-47	11671	19076	139267
GC_Q-48	97283	463690	7740

3.4. Evaluation of the role of local rainwater and groundwater in salt crystallization process

Table S5. Concentrations of anions and cations (mg/L) obtained by ion chromatography in rainwater and groundwater sampled at the Archaeological Park of Pompeii.

	Rainwater	Groundwater
F^-	0.99 ± 0.01	3.0 ± 0.2
Cl^-	9.1 ± 0.3	50 ± 2
NO_3^-	8.7 ± 0.7	81 ± 1
SO_4^{2-}	9.1 ± 0.6	58 ± 1
Na^+	4.67 ± 0.05	28.0 ± 0.2
K^+	6.04 ± 0.01	64.7 ± 0.2
Mg^{2+}	2.98 ± 0.03	24.3 ± 0.1
Ca^{2+}	19.5 ± 0.3	66.9 ± 0.1

3.5. Identification of the main degradation sources causing the crystallization of salts on Pompeian mural paintings

Table S6. Pearson correlation coefficients obtained from the LIBS dataset of the House of Ariadne.

	CaCl	CaF	Na	K
CaCl	1			
CaF	-0.35989	1		
Na	0.20283	0.59359	1	
K	-0.01685	0.51405	0.8519	1

Table S7. Pearson correlation coefficients obtained from the LIBS dataset of the House of the Golden Cupids.

	CaCl	CaF	Na	K
CaCl	1			
CaF	-0.15179	1		
Na	-0.17524	0.09201	1	
K	-0.19131	0.20118	0.89518	1

Table S8. Pearson correlation coefficients obtained from the LIBS net intensities of the dataset of the House of the Golden Cupids after excluding the strong influence of the points associated to restoration mortars.

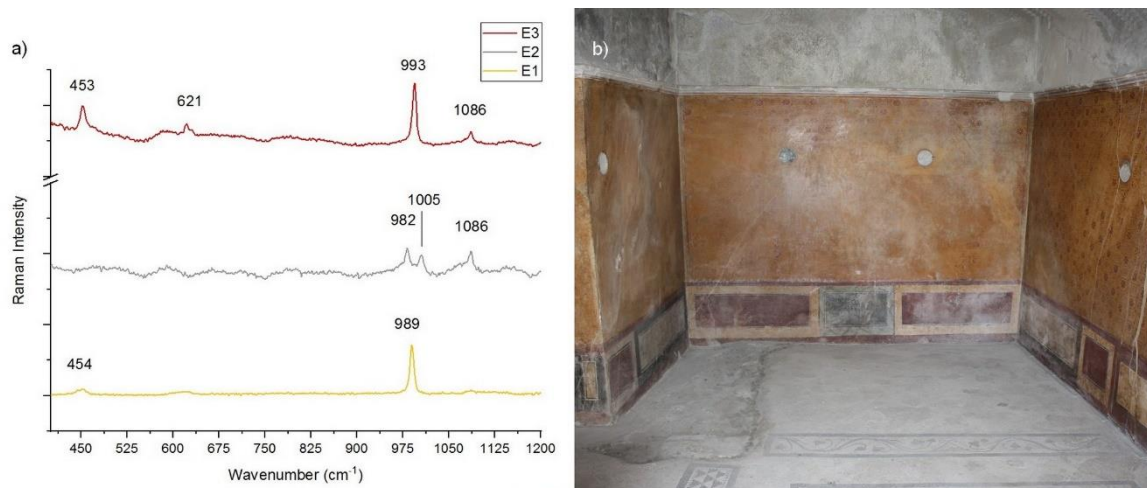|	CaCl	CaF	Na	K
CaCl	1			
CaF	-0.17283	1		
Na	-0.12065	0.34772	1	
K	-0.22893	0.5846	0.79708	1

Fig. S19. A) Raman spectra of points E1 (mirabilite, Raman bands at 454 and 989 cm^{-1}), E2 (syngenite, Raman bands at 982 and 1005 cm^{-1}) and E3 (aphthitalite, 453, 621, 993 and 1086 cm^{-1}; this later Raman band could point to the identification of aphthitalite instead of thenardite and the 993/453 cm^{-1} ratio, close to 2, strongly suggests the identification of aphthitalite instead of thenardite) [5,6]. B) View of Room I (House of the Golden Cupids), where points E1-E3 were analyzed.

REFERENCES

[1] M. Veneranda, N. Prieto-Taboada, S. Fdez-Ortiz de Vallejuelo, M. Maguregui, H. Morillas, I. Marcaida, K. Castro, J.M. Madariaga, M. Osanna, In-situ multianalytical approach to analyze and compare the degradation pathways jeopardizing two murals exposed to different environments (Ariadne House, Pompeii, Italy), Spectrochim. Acta, Part A. 203 (2018). https://doi.org/10.1016/j.saa.2018.05.115.

[2] Pompeii in Pictures, (2021). https://pompeiiinpictures.com/pompeiiinpictures/index.htm (accessed January 19, 2021).

[3] Pompeii Sites Official Pompeii Archaeological Site, (2021). http://pompeiisites.org/en/ (accessed January 19, 2021).

[4] S. Pérez-Diez, L.J. Fernández-Menéndez, H. Morillas, A. Martellone, B.D. Nigris, M. Osanna, N. Bordel, F. Caruso, J.M. Madariaga, M. Maguregui, Elucidation of the Chemical Role of the Pyroclastic Materials on the State of Conservation of Mural Paintings from Pompeii, Angew. Chem. Int. Ed. 60 (2021) 3028–3036. https://doi.org/10.1002/anie.202010497.

[5] N. Prieto-Taboada, S. Fdez-Ortiz De Vallejuelo, M. Veneranda, I. Marcaida, H. Morillas, M. Maguregui, K. Castro, E. De Carolis, M. Osanna, J.M. Madariaga, Study of the soluble salts formation in a recently restored house of Pompeii by in-situ Raman spectroscopy, Sci. Rep. 8 (2018). https://doi.org/10.1038/s41598-018-19485-w.

[6] N. Prieto-Taboada, S. Fdez-Ortiz de Vallejuelo, M. Veneranda, E. Lama, K. Castro, G. Arana, A. Larrañaga, J.M. Madariaga, The Raman spectra of the Na_2SO_4-K_2SO_4 system: Applicability to soluble salts studies in built heritage, J. Raman Spectrosc. 50 (2019) 175–183. https://doi.org/10.1002/jrs.5550.